

Investigation of Radon, Total Electron Content and Linear and Nonlinear Variations of Meteorological Variables Due to Earthquakes: ARIMA and Monte Carlo Modelling

Marjan Mohammed GHAFAR¹, Hemn Salh^{2*}, Fatih Külahcı³

¹ Department of Physics, College of Science, University of Halabja, Halabja, Iraq

² Department of Physics, Faculty of Science and Health, Koya University, Koya KOY45, Iraq

³ Firat University, Science Faculty, Physics Department, Nuclear Physics Division, TR-23119, Elazığ, Harput, Turkey

¹ Marjan.ghafar@uoh.edu.iq, ² hemn.salh@koyauniversity.org, ³ fatihkulahci@firat.edu.tr

(Geliş/Received: 18/01/2023);

Kabul/Accepted: 04/05/2023)

Abstract: An Integrated Autoregressive Moving Average (ARIMA) - Monte Carlo Simulation (MCS) is proposed to analyze and model the anomalies of atmospheric and ground gases by an earthquake along the North Anatolian Fault Zone (Türkiye). Earthquakes, Soil radon gas and Total Electron Content (TEC) showed simultaneous anomalies. There are positive relationships between these three parameters. Also, positive relations between Rn, meteorology, and atmosphere are detected. The proposed ARIMA model and MCS for the Rn-TEC-Earthquake relationships of the measured data gave statistically significant results. This model and simulation showed statistically significant changes in the effects of microearthquakes, which are more difficult to detect than large earthquakes, especially on the ionospheric TEC.

Key words: Total Electron Content, Earthquake precursors, ARIMA, Monte Carlo Simulation

Radon, Toplam Elektron İçeriği ve Meteorolojik Değişkenlerin Depremlere Bağlı Doğrusal ve Doğrusal Olmayan Değişimlerinin İncelenmesi: ARIMA ve Monte Carlo Modellemesi

Öz: Kuzey Anadolu Fay Zonu (Türkiye) boyunca meydana gelen bir depremin atmosferik ve yer gazlarındaki anormallikleri analiz etmek ve modellemek için Entegre Otoregresif Hareketli Ortalama (ARIMA) - Monte Carlo Simülasyonu (MCS) önerilmiştir. Depremler, Toprak radon gazı ve Toplam Elektron İçeriği (TEC) eşzamanlı anormallikler gösterdi. Bu üç parametre arasında pozitif ilişkiler vardır. Ayrıca Rn, meteoroloji ve atmosfer arasında da pozitif ilişkiler tespit edilmiştir. Ölçülen verilerin Rn-TEC-Deprem ilişkileri için önerilen ARIMA modeli ve MCS istatistiksel olarak anlamlı sonuçlar vermiştir. Bu model ve simülasyon, tespit edilmesi büyük depremlere göre daha zor olan mikrodepremlerin, özellikle iyonosferik TEC üzerindeki etkilerinde istatistiksel olarak anlamlı değişiklikler olduğunu gösterdi.

Anahtar kelimeler: Toplam Elektron İçeriği, Deprem öncüleri, ARIMA, Monte Carlo simülasyonu

1. Introduction

Earthquake formations are among the most difficult geological phenomena occurrences that exist on the Earth's surface as a consequence of various parameter influences. Soil radon gas (²²²Rn) alone is insufficient because of the Earth's structure, air pressure, environmental warming, temperature, and interior, among other influences [1–4]. An earthquake is a sudden movement induced by fissures in the Earth's crust [5] and is the result of a large amount of energy moving for heat energy, seismic wave energy, and plastic deformation energy, and then only a seismic wave is considered for the earthquake. The idea of magnitude has been included to make estimating earthquake energy clear [6]. The changes in the composite materials' physical, chemical, and other characteristics that result from the accumulation of stress in the crust are known as the precursors of an earthquake.

Seismologists may detect these actions and use them as a basis for earthquake forecasts [6–9]. While an uncolored gas, radon has a half-life of approximately four days. The most stable isotope of radium that exists is ²²²Rn, the heaviest noble gas. Radium is the primary source of radon in the Earth's crust, Therefore, the amount of radium is mostly equal to the amount of uranium since around 80% of the Rn that is released into the atmosphere is detected in the top few meters of the earth, in rocks and soil. Depending on the type of rock and mineral, different amounts of uranium and radium can be discovered in soil. On average, ²³⁸U is present in 24 Bq/kg of soil worldwide [10]. The study of Rn release rates from the Earth's crust has implications in several fields of earth and atmospheric sciences for quantifying activities ranging from monitoring atmospheric sources to transportation. Radon gas and its offspring can be used. All of this research needs a thorough knowledge of the processes that regulate the amounts of Rn emanation from rocks, minerals, and soil [11]. Rn atoms cannot leave a solid grain due

* Corresponding author: hemn.salh@koyauniversity.org. ORCID Number of authors: ¹ 0000-0002-1343-5594, ² 0000-0002-2367-2980, ³ 0000-0001-6566-4308

to the low solid diffusion coefficients (1×10^{-25} - 1×10^{-27} m²/s) present. It is commonly assumed that parent Ra undergoes radioactive decay and that Rn escapes from the mineral grain as a result of the recoil. Ra decay produces Rn atoms, which frequently escape grains due to recoil and internal space in grains. The molecular diffusion coefficients of air and water can be transmitted by diffusion via processes of Rn removal from the subsurface and subsequent transportation to the atmosphere [12, 13].

For forecasting earthquakes, ²²²Rn has been utilized [14–16], and ²²²Rn has been used for seismic activity monitoring since the Tashkent (M 5.2) earthquake. Six years before the Tashkent earthquake, the study area was considered [17]. As a result, the data also reveals the radon growth rates previous to the earthquake. In many parts of the world, the movement of the Earth's crust has led to new techniques for earthquake prediction [18–20][21–23]. These predicting areas include a variety of strategies with significant effects. These methods include magnetic area, compression, decline, seismic velocity wave, shell resistance, slide down, gravitational effects, and radon measurements, and the data indicate that earthquakes could cause radon levels to increase. There was a significant variance in soil radon gas before the earthquake in Chamoli, India, in 1999 [24, 25], Radon gas was recorded abnormally after the North Indian earthquake of 1997 (M 5.4) due to the observation of an underground water source. Compared to typical soils, radon gas levels are greater [26]. Although the earth's crust typically emits very little radon into the atmosphere, Before the production of volcanic activity and seismic occurrences, fault lines in geothermal in uranium and radon irregularities are seen [27].

Ions and free electrons in the ionosphere, an area of the atmosphere at altitudes between 60 and 1100 km, reflect a small number of electromagnetic waves [28]. The number of free electrons along 1m² of the beam path is represented by atmospheric TEC [29]. The TECU unit, which is used to quantify TEC and is equal to 10¹⁶ electrons.m⁻², is used to directly investigate the ionosphere's composition [30]. The recipient's zenith and Slant Total Electron Content are used to determine the recipient's free electron content in the slant line between the receiver and the satellite. Using Vertical TEC, TEC is measured (STEC) [31]. The ionosphere can be affected by geomagnetic forces, diurnal and seasonal influences, solar interference, and earthquakes, which result in irregularities in the ionosphere [32]. Because that can account for ionosphere changes caused by this activity, the TEC is an essential study factor for the relation between pre-earthquake and seismic activities. This is because the Earth's crust has experienced seismic and pre-earthquake events that stress rocks. Stresses cause the positive electrical charge of stones inside the crust of the earth. When positive charges develop, they generate a potential difference on the outer surfaces of the stones, which generates a charge transfer that may travel quickly and thus be away from its source position. Charges flow upward due to the operation of the electric field lines between the Earth's crust and the ionosphere's bottom. It reached the ionosphere's bottom due to a change in the ionosphere's electron equilibrium [33]. If TEC disruptions might be used to direct earthquake monitoring, such a disturbance in total electron content also may signal significant seismic prediction, where these disruptions might be used in an earthquake predicting system to improve earthquake alert systems, thus saving hundreds of lives [34]. Ionosphere abnormalities are caused by earthquakes, solar interference, seasonal and diurnal impacts, and geomagnetic influences, among other factors [35, 36]. Ionospheric changes have been detected as earthquake precursors in more than 20 nations [37, 38].

This research aims to estimate the formation of radon gas in soil which is closely related to seismic events, as well as variations in ionospheric TEC while accounting for earthquakes, and to correlate together utilizing Monte Carlo Simulation. Some meteorological factors are also taken into account while analyzing this relation. The results revealed significant conclusions about the TEC-Rn-Earthquake triad co-change.

2. Analysis of data and the Study Area

One of the countries with the most seismic activity is Türkiye, It is seismically affected by The North Anatolian Activity Zone (NAFZ), which affects the region's north while causing a 1,600 km-long surface rupture for dextral strike-slip movement, The place is located on the North Anatolian Fault's eastern side and serves as a research location, and this is an important region in terms of development and future expansion due to earthquake disasters in 1942 and 1943, with magnitudes of 7.6 and 7.2, respectively [32, 39, 40]. Türkiye's Tokat Province's research district is known as Yolkonak. This region is located near the NAFZ, one of Türkiye's major fault zones. The Tokat Region and the middle Black Sea are where the NAFZ is situated. It covers the area between north latitude and (longitude 36o.89443, latitude 40o.53932). The topographic maps are illustrated in Figure 1.

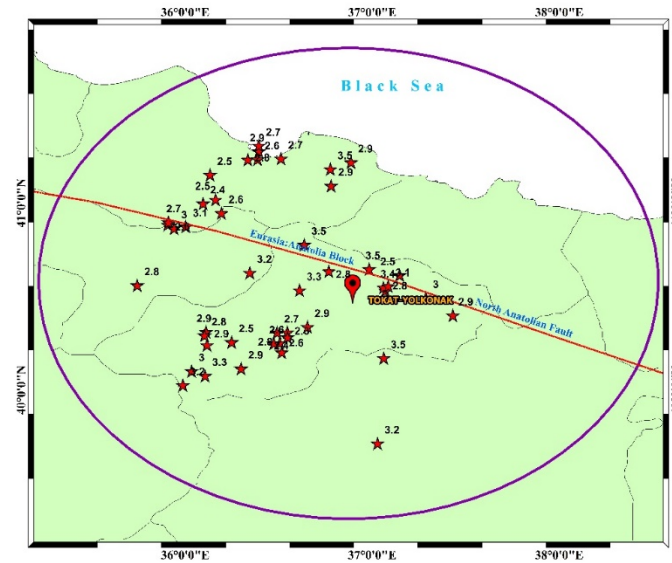


Figure 1. The exact location of the radon monitoring station and studied earthquakes along the North Anatolian Fault zones in T rkiye.

The data for the ^{222}Rn time series was provided by the Government of T rkiye Ministry of Interior's Emergency and Disaster Management Agency (AFAD) [41]. From 4 March 2007 to 10 February 2010, soil radon was monitored using an alpha particle detector at approximately one meter deep in the soil at 15-minute intervals. Alpha Nuclear Corporation, Canada, created the detecting, version 611-Alpha Meter Assume a 400 mm² stainless steel silicon diffusing cross-detector container with an aluminium Mylar covering [42]. The sensing surface of the detector is 450 mm². Because this detection works much better in a dark, dry environment, it is enclosed beneath a thin opaque film or membrane. Since the film is 0.25 mm thick and made of aluminized Mylar, it has a sufficiently low density to allow for the efficient transit of alpha particles in addition to water vapour and light. The TR Meteorology General Directorate offers daily mean steam pressure (hPa), dry bulb temperature, wet bulb temperatures, and soil temperature at deeper distances of 10, 20, and 50 cm to examine the influence of meteorological parameters on the ^{222}Rn during the observation period [43]. The seismic data were collected by Bogazici University, Kandilli Center, and the Earthquake Research Institute [44]. Furthermore, the regularized estimate procedure for GPS data was used in this study to generate three mid-latitude stations' VTEC values, Istanbul, (41.06N, 29.01E), Ankara, (39.53N, 32.45E), and Gebze (40.47N, 29.27E), via Laboratory for Ionosphere Research (IONOLAB)[45] [46–52].

3. Result and Discussion

3.1 Monte Carlo Modeling and the Autoregressive Integrated Moving Average Method

The (ARIMA) Autoregressive Integrated Moving Average prediction test is utilized for predicting. Several times preceding terms should be taken into account and expressed as a series of different models depending on the time series model. A MATLAB application is utilized to evaluate whether seismic activity in the study region could be the cause of any radon data anomalies. It provides a workstation for developing the ideal ARIMA model through Monte Carlo simulations to predict future radon time series. To select the best ARIMA model, 80 percent of the total Rn data is imported and used as the train data set. The remaining 20 percent is then used to evaluate the Monte-Carlo simulation data prediction. The ARIMA model can be used only with stationary data (45,46]. Because the Rn train data set's t-static is higher than the crucial value and is thus deviated by one degree. The partial autocorrelation function (PACF) and autocorrelation functions (ACF) indicate that the data are stationary. The moving average q orders and autoregressive p orders may also be found using the ACF and PACF plots. As shown in Figure 2. Initially, train data is used to apply ARIMA (p, d, q). The chosen time series model is thus ARIMA (4,1,13), which has the formula given in (1):

$$(1 - \phi_1 L - \dots - \phi_4 L^4)(1 - L)y_t = C + (1 + \theta_1 L - \dots - \theta_{13} L^{13})\varepsilon_t, \quad (1)$$

In this equation, ϕ and θ and are the model's input parameters, ε_t represents the error at time t and C is a constant amount.

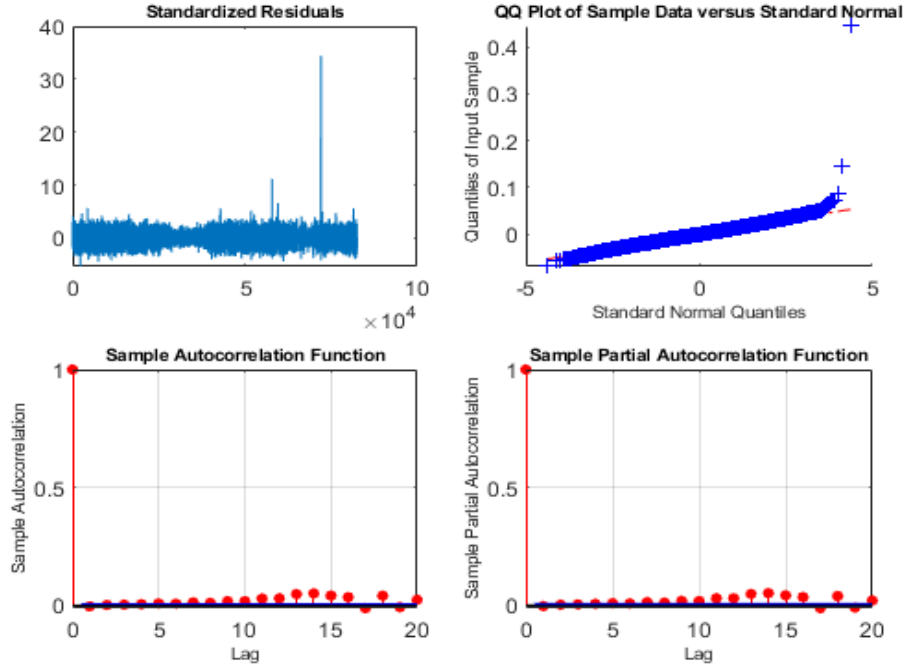


Figure 2. Partial autocorrelation function and autocorrelation function plots (lower part); the standardized residuals and the quantile-quantile of the ARIMA model residuals (upper part).

Figure 2 shows the histogram of the model's residuals, which shows that they follow the standard distribution, and the accuracy of the fitted model's residues is examined. Figure 2 shows the q-q plot of the model's residuals. It can be seen that there appear to be irregularities despite a few minor tail variances. The normal distribution's value and both residues' values combined, indicate that ARIMA (4,1,13) is an appropriate model.

MCS is a mathematical approach to decision-making and statistical analysis. It is useful in many fields, including nuclear energy, engineering, high-energy physics and atomic, research and development, the environment, and transportation [56–59]. It identifies the best with worst situations in all possible outcomes and displays all possible outcomes with each option, typically using probabilities (PDF) [60] as well as how to apply these inputs to the distribution MCS performs multiple analyses and, A PDF indicates that this helps in providing a range of potential outcomes based on the number of uncertainties as well as the range of input values associated with such uncertainties. The usage of PDFs, which can take several forms like Gaussian, lognormal, or uniform, is the most sensible and trustworthy method for defining uncertainties in a risk modelling job. Randomly calculated probability distribution functions (PDFs) are used to sample data during MCS. Each sample set's iteration is specified, and the data is provided as displayed in this data sample. The MCS technique displays not just potential outcomes but also information on the PDFs that these outcomes produce [61, 62]. The Monte-Carlo simulation tries four distinct pathways and forecasts 20% of data time steps based on the ARIMA model. It appears suitable, as demonstrated in Figure 3, which also shows the Monte-Carlo forecast probability boundaries. The red lines represent lower and higher limits, the green lines represent radon, and the black line indicates the Monte Carlo average.

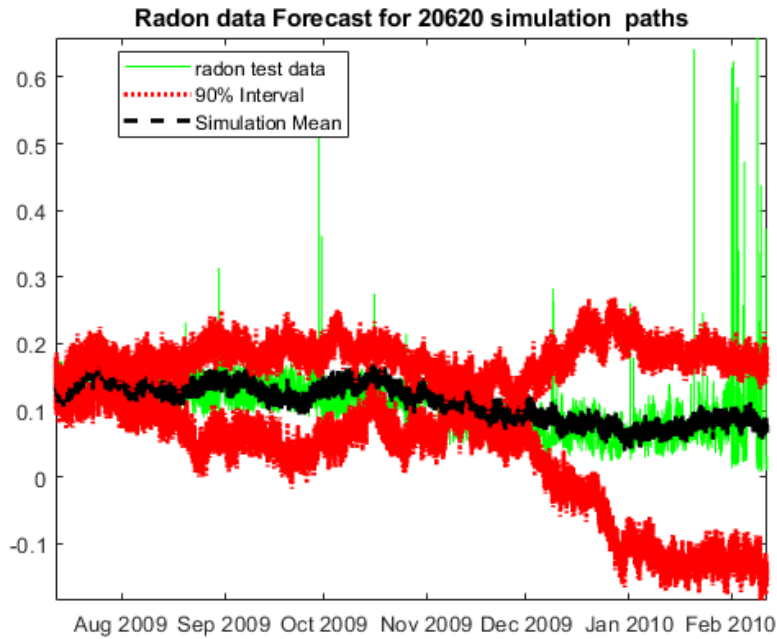


Figure 3. The mean of Monte Carlo Simulation Rn forecasts with lower and upper bounds.

3.2 Non-Seismic Related Variations in Radon Gas Concentration in Soil and Air

Figure 4 shows the radon time series analyzed between March 2007 and February 2010. It has been shown that the Rn concentration varies over time. There is no notable variation in the radon level from the beginning of March to the end of November 2007; therefore, its concentration varies around this standard ($150 \text{ Bq} \cdot \frac{1}{\text{m}^3}$). As a result, the Rn level began to fall progressively beginning in mid-October.

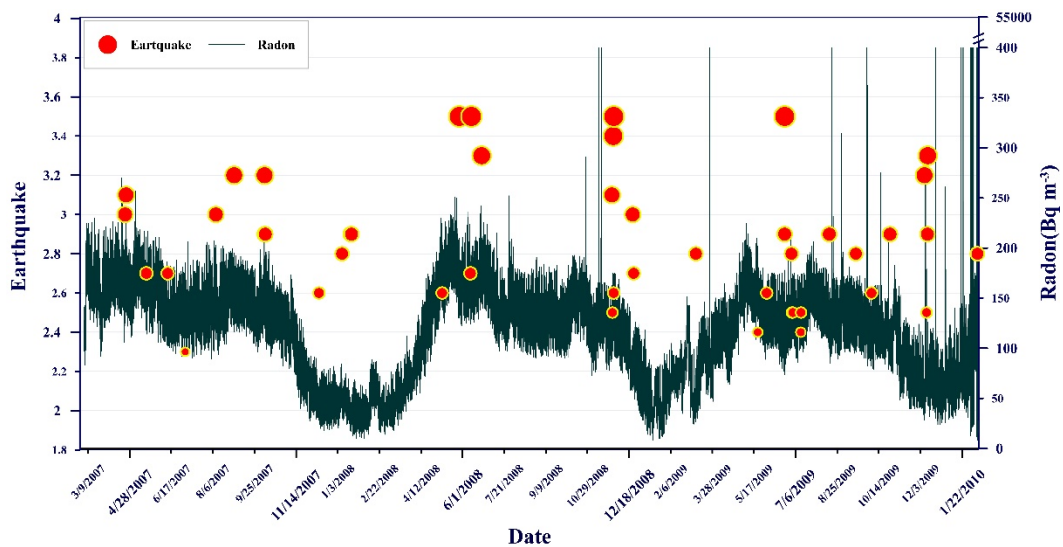


Figure 4. The studied Rn time series data.

In comparison to the end of 2007, when the Rn content reached its lowest concentration of around ($150 \text{ Bq} \cdot \frac{1}{\text{m}^3}$), the Rn concentration fluctuations in December 2007, January, and February 2008 are insignificant.

The Rn level progressively rose to start in March 2008, with spring being the time of year with the maximum Rn concentration. Until the end of the summer, there was a high concentration of Rn, which progressively lowered until the 2009 winter. The seasonal cycle of soil air Rn concentrations may continue until 2010. This variation in Rn concentration is seasonal. Vertical fissures in the clay open up throughout the summer due to increased permeability and Rn concentrations [63]. Earthquake stress in the earth's crust has a considerable influence on Rn emission. Rn gas flow has also been observed to be influenced by temperature variations between soil and air. At temperatures below $-10\text{ }^{\circ}\text{C}$, Rn may be extracted from an air stream for activated charcoal, cooling to liquid N_2 on glass wool at $-196\text{ }^{\circ}\text{C}$, and soil CO_2 at $-78.5\text{ }^{\circ}\text{C}$. Rn condenses on the surface at around $-150\text{ }^{\circ}\text{C}$ even though the partial pressure of soil ^{222}Rn is quite low in environmental conditions [64]. Due to the inverse relationship between temperature and relative humidity in the air, the rising surface soil moisture content is connected to higher air and soil temperatures. In comparison to lower temperatures, higher Rn emanation levels are expected [65].

Variations in air pressure are a result of flux from the Earth's atmosphere on the ground [64]. Frontal system routes are associated with 1%-2% pressure fluctuations, which are thought to have resulted in 20–60% variances in ^{222}Rn flux on the earth's surface [66]. High indoor Rn levels are generally attributed to a pressure difference between the basement and the rest of the residence. Most buildings have high levels of indoor radon, which is caused by the living area/basement pressure differential. The lower basement pressure creates a suction effect. Since the air pressure at the surface is greater than the air pressure at the ground level, Rn gas must be released into the atmosphere [65].

3.3 Possible Seismic Activity Associated Variations in Soil-Air Radon Gas Concentration

During the years 2007-2010, earthquake activity in the research region of Tokat province was documented by Bogazici University, Kandili Observatory, and the Research Center for Seismic. It has been discovered that there are around 45 earthquakes with magnitudes ranging from 2.3 ML and 3.5 ML. As shown in Figure 5, The earthquakes are related to the time-series data in which the radon data are collected, and the seismic data are related to the Rn concentration.

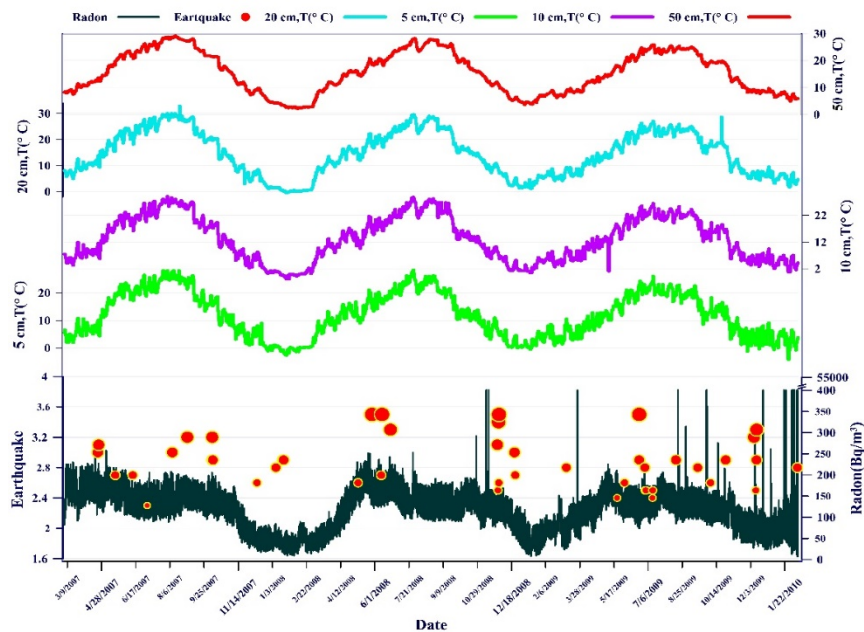


Figure 5. The variations of the radon concentration with soil temperature at (5, 10, 20, and 50 cm) depths.

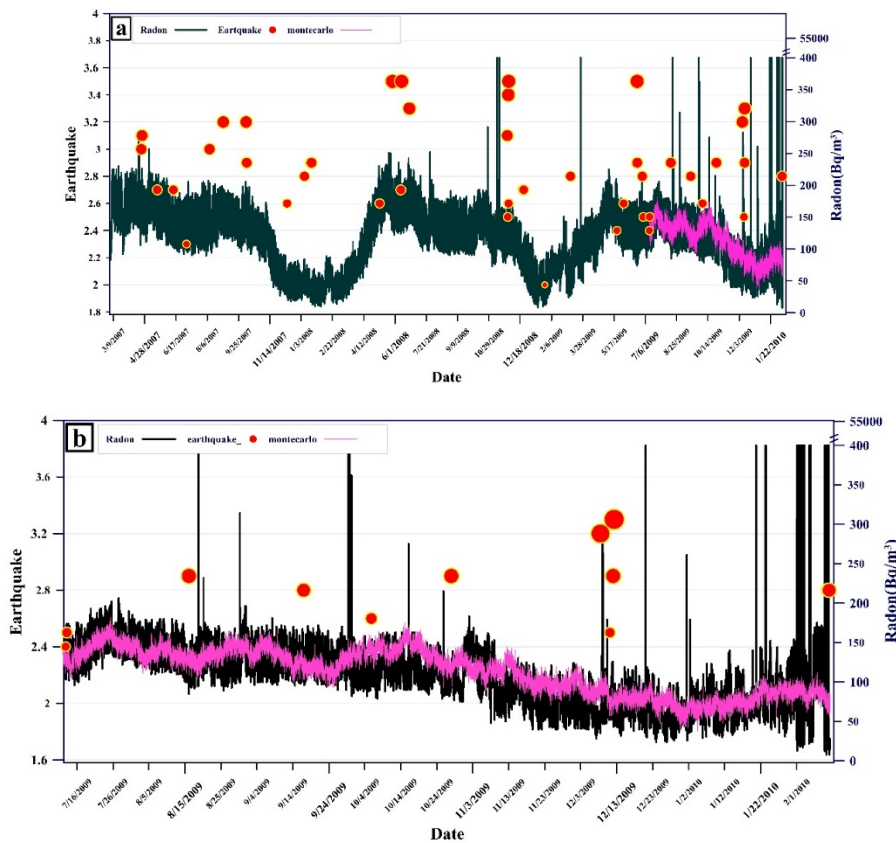


Figure 6. (a) The training and evaluation parts of the radon data with all earthquakes in the study area, (b) The MCS forecasted radon data.

Seven of these occurred in 2007, with the largest having a magnitude of 3.2 ML. There is some variance in radon concentration. As a result, the previously indicated seasonal variance occurred. In 2008, there were about 14 earthquakes, three of which had magnitudes of ML=3.4, and 3.5, 3.5 in July and May, respectively, in Sehitler-(Tokat) [South East 0.9 km], Mescitkoy-Almus (Tokat) [South 5.0 km], and in Gokal-Erbaa (Tokat) [South West 4.5 km], Rn levels reached their peak a month following these earthquakes. All of these factors influence Rn release from the earth's surface [67]. The largest number of Rn disturbances and eighteen earthquakes were recorded in 2009. When compared to other locations, the seismic distance was then closer. In the studied region in 2010, there were just two earthquakes recorded. Figure 5 shows the relation between Rn and soil temperature. Subsurface drilling, gas releases, tensions, earthquakes, and volcanic eruptions, all of these factors influence Rn release from the earth's surface, among other geochemical and geophysical factors. The link between Rn fluctuations and atmospheric and weather changes is shown reasonably in Figure 5.

3.4 Radon anomaly detection using Monte Carlo Simulation

Figure 6(a) shows how the radon data is split into a "train" set of 80 percent for use in determining the best ARIMA model and a "test" set of 20 percent for use in measuring the accuracy of the MCS data prediction. Figure 6 (a) begins with two 2.4 and 2.5 micro-earthquakes. Due to the minor earthquakes, radon didn't change significantly. Later, on August 15, 2009, as a result of these earthquakes, there were two Rn irregularities, parallel to Rn is the Monte Carlo line. The fourth seismic event, measuring 2.9 magnitudes, occurred on September 16, 2009. The Rn concentration didn't increase immediately after the earthquake, but it did grow over time. Following the occurrence of these earthquakes' Rn anomalies, four earthquakes occurred in December 2009. Soil permeability shows that seismic fault lines, geothermal sources, uranium resources, and other potential energy sources are all present in the Anatolian Fault Zone, where the research was conducted and volcanic zones are theoretically specified, the Rn concentration increases. Rock, soil, mineral, and uranium mine tailings all naturally emit radon

^{222}Rn into the surrounding environment. Higher levels of Rn emission occur at warmer air and soil temperatures than at cooler ones, resulting in a positive Rn anomaly when the exposed moisture content temperature rises. Significant factors include the magnitude of the earthquake and the distance from the epicentre. The magnitude of the earthquake and its distance from the monitoring station have a significant impact on the peak intensity and width of the Rn anomaly.

3.5 Variations in the ionospheric Total Electron Content (TEC)

TEC is an essential study measure because it may explain ionosphere changes caused by pre-earthquake and seismic events. For three locations in the research region, Figure 7 shows the temporal radon with total electron. Figure 7 shows the findings of a triple examination of earthquake-TEC and Rn Anomalies. As an example, one may study this figure from the perspectives of numerous basic components. On the other hand, the number of these parts can be increased (similar to the variations during 2007 and 2008), Earthquake-Rn-TEC causes abnormalities very instantly, according to analysis. In the red column, the Rn gas concentration in the soil is seen to have been released as a consequence of several earthquakes. The blue and yellow columns illustrate this, similar fill-discharge trends are seen. For all three TEC stations, these abnormalities usually show consistent behaviour.

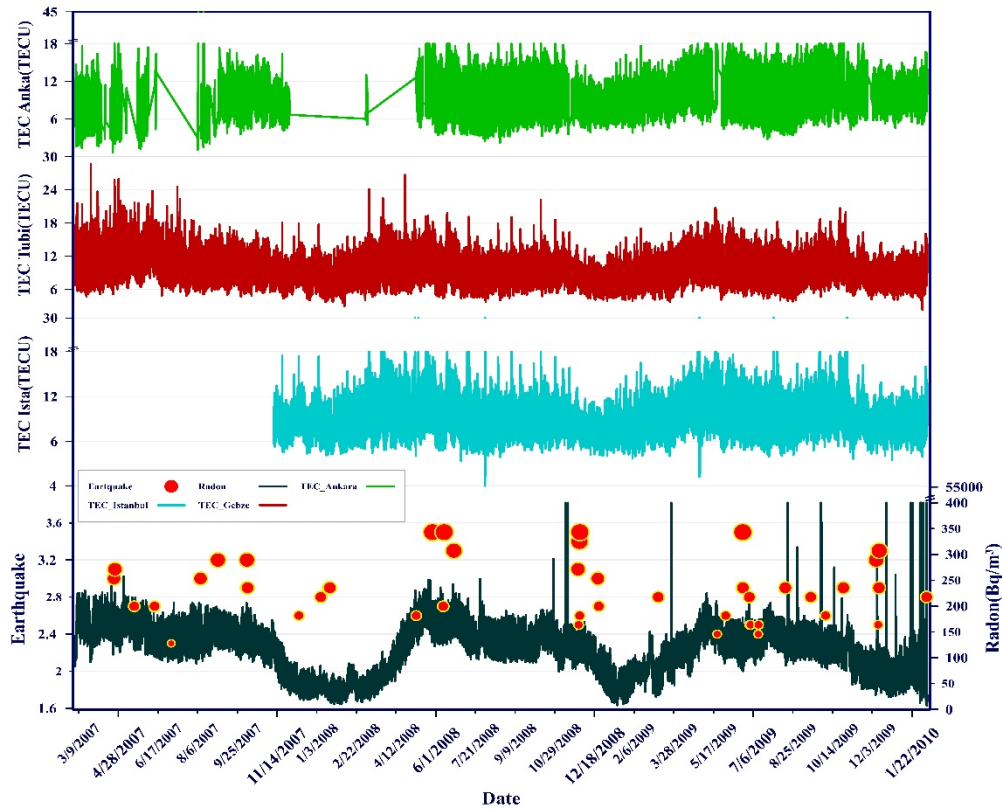


Figure 7. Radon time series, earthquake magnitude, and total electron content for three stations Tubi (Gebze), Ista (Istanbul), Anka (Ankara).

The graph did not begin at the origin since there is missing data from November 2007 until the start of the green line, which represents the TEC in the Ista station in Istanbul. the Tubi (Gebze) station's total electron content during the previous study period is represented by the purple line. The total content is shown as a brown line. In Anka (Ankara) station, the electron data was interrupted in 2007 and resumed in 2008. The limits by the standard deviation of the equation given, applied 10 days before and 5 days after the observation day, are used to determine whether the daily TEC result is within confident intervals of average and standard deviation, see the equations (2) and (3) as follows:

$$\text{Upper Bound} = \text{mean} + 2 \text{ stdev}, \quad (2)$$

$$\text{Lower Bound} = \text{mean} - 2 \text{ stdev}, \quad (3)$$

Figure 8(a) demonstrates that the anomaly at the three stations is comparable. Due to three days of TEC abnormalities at the Ista-station before and after the earthquake variation, shows a TEC anomaly that was discovered five days before the earthquake measuring 2.8 on the Richter scale on September 16, 2009. Predictions made using both Rn concentration and MCS tend to be accurate. Figure 8(b) shows the M_L 3.2 earthquake that occurred on December 7, 2009, on the Richter scale. Three days before the earthquake and immediately following it, TEC anomalies were seen with decreasing TEC values. While the daily fluctuations in Rn concentration before the earthquake were greater than the fluctuations seen afterwards, some Rn anomalies persisted. Although the Monte Carlo line and radon are nearly parallel, so often, it is not reasonable. As shown in Figure 8(b), on December 11, 2009, a most latest earthquake was 3.0 on the Richter scale. Nevertheless, forty-eight hours later, the quantity of TEC increased for three days, seemingly unrelated to the seismic. The intense seismic activity may have caused the abnormally large number of electrons to indicate a GPS signal that can be received at a greater distance from the epicenter. The TEC irregularity shows that there may be background noise blocking GPS signals in the high atmosphere under the influence of the generating force from the region surrounding the epicenter [68]. This might be caused by magnetic storms and solar, and plasma level concentration indicates that significant ionosphere irregularities are often associated with plasma upward drift near seismogenic locations [69].

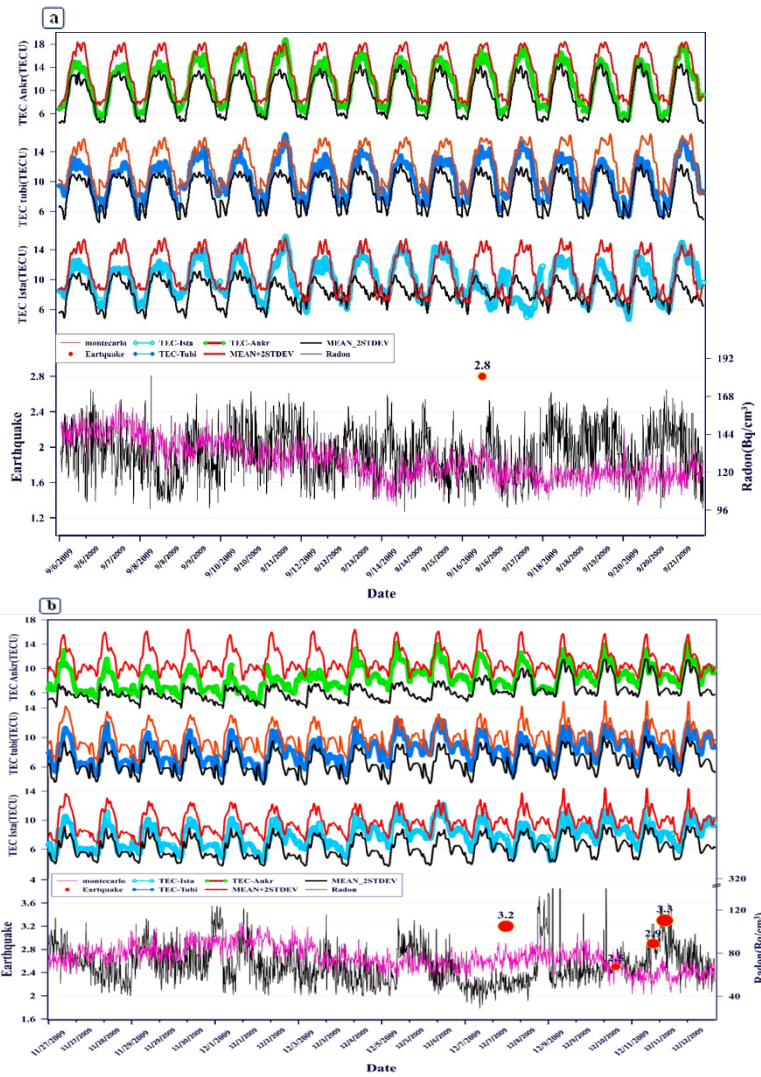


Figure 8 (a) TEC and radon variation before and after an earthquake ML 2.9 on September 16, 2009, (b) TEC and radon variation before and after an earthquake ML 3.2 on December 7, 2009.

4. Conclusions

In Yolkonak/Tokat, Türkiye, the study examined changes in Rn content in soil gas over around four years. At a depth of 1 m, fluctuations in the radon concentration have been seen that are both seasonal and non-seasonal. Regarding seasonal fluctuations, wintertime appears to have the lowest Rn concentration, It is increased in the summer because of the effects of meteorological factors on radon transport typical processes such as diffusion. Before the August and December 2009 microearthquakes, Monte Carlo simulations with growing radon levels revealed non-seasonal variations (anomalies). The North Anatolian Fault Zone (NAFZ) earthquake may be anticipated by these anomalies. In these situations, variations in the total amount of electrons in the ionospheric atmosphere seem to be linked to radon anomalies. For instance, Rn levels increased and total electron concentration exceeded upper boundaries before the earthquake on December 12, 2009. However, the MCS method generates the PDF by calculating using all available data, unlike interpreting a single variable, resulting in optimal simulation optimization. When MCS is applied in combination using the Model (ARIMA), statistical outputs with high reliability are created with high reliability. Using the ARIMA-MCS approach in data interpretation is useful for this study. We advocate for the application of various artificial intelligence approaches in various investigations. Similar to the investigation of soil Rn gas time series, warmer seasons are characterized by much greater positive rises in Rn anomalies than cold ones. These rises are caused by a decrease in moisture during hotter seasons, the rise in temperature causes soil pores to expand and the spaces between soil particles to grow, the Moon's gravitational movements have a positive influence on soil, a decrease in rainfall, and the resulting dryness. These seasonal fluctuations are useful for measuring earthquake-Rn change. Rn surface changes are directly influenced by variations in air pressure. Rn is positively correlated with both meteorological changes and atmospheric changes. Rn-TEC and Earthquakes have a positive correlation.

Acknowledgments

We would like to thank Boğaziçi Kandilli Observatory (<http://www.koeri.boun.edu.tr/scripts/lasteq.asp>) for earthquake data, AFAD (Ministry of Interior Disaster and Emergency Management Presidency, <https://en.afad.gov.tr/>) for Rn data, IONOLAB (<http://www.ionolab.org/index.php?page=index&language=en>) for TEC data, TR Meteorology General Directorate (<https://www.mgm.gov.tr/eng/forecast-cities.aspx>) for meteorology data.

References

- [1] Külahci F, Inceöz M, Doğru M, Aksoy E, Baykara O. Artificial neural network model for earthquake prediction with radon monitoring. *Applied Radiation and Isotopes*. 67, 212-219 (2009). <https://doi.org/10.1016/J.APRADISO.2008.08.003>
- [2] Anisimov SV, Dmitriev EM, Aphinogenov KV, Guriev AV, Kozmina AS. Variability of radon distribution in the atmospheric surface layer over the land of middle latitudes. *IOP Conf Ser Earth Environ Sci*. 231, (2019). <https://doi.org/10.1088/1755-1315/231/1/012006>
- [3] Kulali F, Akkurt I, Özgür N. The effect of meteorological parameters on radon concentration in soil gas. *Acta Phys Pol A*. 132, 999-1001 (2017). <https://doi.org/10.12693/APhysPolA.132.999>
- [4] Fuente M, Rábago D, Goggins J, Fuente I, Sainz C, Foley M. Radon mitigation by soil depressurisation case study: Radon concentration and pressure field extension monitoring in a pilot house in Spain. *Science of the Total Environment*. 695, (2019). <https://doi.org/10.1016/j.scitotenv.2019.133746>
- [5] MILNE J. The California Earthquake of April 18, 1906. *Nature* 1910 84:2128. 84, 165-166 (1910). <https://doi.org/10.1038/084165a0>
- [6] Pulnests S. *The Possibility of Earthquake Forecasting: Learning from nature*. IOP Publishing Ltd 2018 (2018)
- [7] Mahmood I, M.F. Shahzad MI, Qaiser S. Investigation of atmospheric anomalies associated with Kashmir and Awaran Earthquakes. *J Atmos Sol Terr Phys*. 154, 75-85 (2017). <https://doi.org/10.1016/j.jastp.2016.12.018>

- [8] Huang F, Li M, Ma Y, Han Y, Tian L, Yan W, Li X. Studies on earthquake precursors in China: A review for recent 50 years, (2017)
- [9] Akyol AA, Arikan O, Arikan F. A Machine Learning-Based Detection of Earthquake Precursors Using Ionospheric Data. *Radio Sci.* 55, (2020). <https://doi.org/10.1029/2019RS006931>
- [10] Nazaroff WW. Radon transport from soil to air. *Reviews of Geophysics.* 30, 137-160 (1992). <https://doi.org/10.1029/92RG00055>
- [11] Hosoda M, Tokonami S, Suzuki T, Janik M. Machine learning as a tool for analysing the impact of environmental parameters on the radon exhalation rate from soil. *Radiat Meas.* 138, (2020). <https://doi.org/10.1016/J.RADMEAS.2020.106402>
- [12] Ye Q, Singh RP, He A, Ji S, Liu C. Characteristic behavior of water radon associated with Wenchuan and Lushan earthquakes along Longmenshan fault. *Radiat Meas.* 76, 44-53 (2015). <https://doi.org/10.1016/j.radmeas.2015.04.001>
- [13] Rikitake T. Predictions and precursors of major earthquakes: the science of macro-scopic anomalous phenomena. Terra Scientific Publishing Company (2001)
- [14] Rikitake T. Earthquake prediction. *Earth Sci Rev.* 4, 245-282 (1968). [https://doi.org/https://doi.org/10.1016/0012-8252\(68\)90154-2](https://doi.org/https://doi.org/10.1016/0012-8252(68)90154-2)
- [15] Birchard GF, Libby W.F.: Soil radon concentration changes preceding and following four magnitude 4.2–4.7 earthquakes on the San Jacinto Fault in southern California. *J Geophys Res Solid Earth.* 85, 3100-3106 (1980)
- [16] King CY. Radon emanation on San Andreas Fault. *Nature* 1978 271:5645. 271, 516-519 (1978). <https://doi.org/10.1038/271516a0>
- [17] Ulomov VI, Zakharova A.I., Nauk N.V.U.-D.A., undefined 1967. The Tashkent earthquake of April 26, 1966, and its repeated shocks. mathnet.ru.
- [18] Kūlahcı F, Zeki Ş. On the Correction of Spatial and Statistical Uncertainties in Systematic Measurements of ²²²Rn for Earthquake Prediction. *Geophysics* . 35, 449-478 (2014). <https://doi.org/10.1007/s10712-013-9273-8>
- [19] Tse ST, Rice JR. Crustal earthquake instability in relation to the depth variation of frictional slip properties. *J Geophys Res.* 91, 9452 (1986). <https://doi.org/10.1029/jb091ib09p09452>
- [20] Muhammad A, Kūlahcı F, Salh H, Hama RA. Long Short Term Memory networks (LSTM)-Monte-Carlo simulation of near surface ionization using radon. *J Atmos Sol Terr Phys.* (2021). <https://doi.org/10.1016/j.jastp.2021.105688>
- [21] Wattanakorn, K, Wiboolsake S. Soil gas radon as an earthquake precursor: Some considerations on data improvement. *Radiat Meas.* 29, 593-598 (1998). [https://doi.org/10.1016/S1350-4487\(98\)00079-1](https://doi.org/10.1016/S1350-4487(98)00079-1)
- [22] Ghosh D, Deb A, Sengupta R, Patra KK, Bera S. Pronounced soil-radon anomaly-Precursor of recent earthquakes in India. *Radiat Meas.* 42, 466-471 (2007). <https://doi.org/10.1016/j.radmeas.2006.12.008>
- [23] Kuo T, Su C, Chang C, Lin C, Cheng W, Liang H, Lewis C, Chiang C. Application of recurrent radon precursors for forecasting large earthquake near Antung, Taiwan. *Radiat Meas.* 45, 1049-1054 (2010). <https://doi.org/10.1016/j.radmeas.2010.08.009>
- [24] Singh M, Kumar M, Jain R, Chatrath R. Radon in ground water related to seismic events. (2019)
- [25] Virk, Walia HS. Helium/radon precursory signals of Chamoli Earthquake, India. *Radiat Meas.* 34, 379-384 (2001). [https://doi.org/https://doi.org/10.1016/S1350-4487\(01\)00190-1](https://doi.org/https://doi.org/10.1016/S1350-4487(01)00190-1)

- [26] Viñas R, Darwich A, Soler V, Martín-Luis MC, Quesada ML, de la Nuez J. Processing of radon time series in underground environments: Implications for volcanic surveillance in the island of Tenerife, Canary Islands, Spain. *Radiat Meas.* 42, 101-115 (2007). <https://doi.org/10.1016/j.radmeas.2006.07.002>
- [27] Kūlahci F, Inceöz M, Dođru M, Aksoy E, Baykara O. Artificial neural network model for earthquake prediction with radon monitoring. *Applied Radiation and Isotopes.* 67, 212-219 (2009). <https://doi.org/10.1016/J.APRADISO.2008.08.003>
- [28] Inyurt S, Peker S, Mekik C. Monitoring potential ionospheric changes caused by the Van earthquake (<i>M</i> <sub>w</sub> > 7.2). *Ann Geophys.* 37, 143-151 (2019). <https://doi.org/10.5194/angeo-37-143-2019>
- [29] Arikan F, Arikan O, Erol CB. Regularized estimation of TEC from GPS data for certain midlatitude stations and comparison with the IRI model. *Advances in Space Research.* 39, 867-874 (2007). <https://doi.org/10.1016/j.asr.2007.01.082>
- [30] Géodésique, des sciences naturelles. C. Mapping and predicting the Earth's ionosphere using the Global Positioning System. (1999)
- [31] Langley, RB. Monitoring the Ionosphere and Neutral Atmosphere with GPS.
- [32] Inyurt S, Peker S, Mekik C. Monitoring potential ionospheric changes caused by the Van earthquake . *Ann Geophys.* 37, 143-151 (2019). <https://doi.org/10.5194/angeo-37-143-2019>
- [33] Viti M, Mantovani E, Cenni N, Vannucchi A. Interaction of seismic sources in the Apennine belt. *Physics and Chemistry of the Earth, Parts A/B/C.* 63, 25-35 (2013). <https://doi.org/10.1016/j.pce.2013.03.005>
- [34] Hammerstrom JA, Cornely PR. Total Electron Content (TEC) Variations and Correlation with Seismic Activity over Japan. (2016). <https://doi.org/10.22186/JYI.31.4.13-16>
- [35] Namgaladze AA, Zolotov OV, Karpov MI, Romanovskaya YV. Manifestations of the earthquake preparations in the ionosphere total electron content variations. *Nat Sci (Irvine).* 4, 848-855 (2012). <https://doi.org/10.4236/NS.2012.411113>
- [36] Li M, Parrot M. Statistical analysis of the ionospheric ion density recorded by DEMETER in the epicenter areas of earthquakes as well as in their magnetically conjugate point areas. *Advances in Space Research.* 61, 974-984 (2018). <https://doi.org/10.1016/j.asr.2017.10.047>
- [37] Liu J.Y., Chen C.H., Chen Y.I., Yang W.H., Oyama K.I., Kuo K.W. A statistical study of ionospheric earthquake precursors monitored by using equatorial ionization anomaly of GPS TEC in Taiwan during 2001-2007. *J Asian Earth Sci.* 39, 76-80 (2010). <https://doi.org/10.1016/j.jseaes.2010.02.012>
- [38] Li M, Parrot M. Statistical analysis of the ionospheric ion density recorded by DEMETER in the epicenter areas of earthquakes as well as in their magnetically conjugate point areas. *Advances in Space Research.* 61, 974-984 (2018). <https://doi.org/10.1016/j.asr.2017.10.047>
- [39] Şengör AMC, Zabcı C. The North Anatolian Fault and the North Anatolian Shear Zone. *World Geomorphological Landscapes.* 481-494 (2019). https://doi.org/10.1007/978-3-030-03515-0_27
- [40] Allen CR. Active Faulting in Northern Turkey. (1969)
- [41] Ministry of interior DAEMP. Disaster And Emergency Coordination Board, <https://en.afad.gov.tr/disaster-and-emergency-coordination-board>
- [42] Thomas D.M., Cotter J.M., Holford D. Experimental design for soil gas radon monitoring. *Journal of Radioanalytical and Nuclear Chemistry Articles.* 161, 313-323 (1992). <https://doi.org/10.1007/BF02040478>

- [43] Turkish State Meteorological Service Official Web Sites, <https://www.mgm.gov.tr/eng/forecast-cities.aspx>
- [44] Boğaziçi University. Earthquake Catalog - BOUN KOERI Regional Earthquake-Tsunami Monitoring Center, <http://www.koeri.boun.edu.tr/sismo/2/earthquake-catalog/>
- [45] Sezen U, Arikan F, Arikan O, Ugurlu O, Sadeghimorad A. Online, automatic, near-real time estimation of GPS-TEC: IONOLAB-TEC. *Space Weather*. 11, 297-305 (2013)
- [46] Arikan F, Deviren MN, Lenk O, Sezen U, Arikan O. Observed Ionospheric Effects of 23 October 2011 Van, Turkey Earthquake. *Geomatics, Natural Hazards and Risk*. 3, (2012). <https://doi.org/10.1080/19475705.2011.638027>
- [47] Tuna H, Arikan O, Arikan F. Model based Computerized Ionospheric Tomography in space and time. *Advances in Space Research*. 61, (2018). <https://doi.org/10.1016/j.asr.2018.01.031>
- [48] Arikan F, Sezen U, Toker C, Artuner H. Improved IONOLAB-TEC Space Weather Service GIM-TEC. (2015)
- [49] Gulyaeva TL, Arikan F, Stanislawska I. Earthquake aftereffects in the Equatorial Ionization Anomaly region under geomagnetic quiet and storm conditions. *Advances in Space Research*. 60, 406-418 (2017). <https://doi.org/10.1016/j.asr.2017.03.039>
- [50] Deviren MN, Arikan F. IONOLAB-MAP. An automatic spatial interpolation algorithm for total electron content. *Turkish Journal of Electrical Engineering and Computer Sciences*. 26, 1933-1945 (2018). <https://doi.org/10.3906/elk-1611-231>
- [51] Karatay S, Arikan F, Arikan O. Investigation of total electron content variability due to seismic and geomagnetic disturbances in the ionosphere. *Radio Sci*. 45, (2010). <https://doi.org/10.1029/2009RS004313>
- [52] Arikan F, Shukurov S, Tuna H, Arikan O, Gulyaeva TL. Performance of GPS slant total electron content and IRI-Plas-STECh for days with ionospheric disturbance. *Geod Geodyn*. 7, 1-10 (2016). <https://doi.org/10.1016/j.geog.2015.12.009>
- [53] Salh H, Kūlahcı F, Aközcan S. A mobile simulation and ARIMA modeling for prediction of air radiation dose rates. *Journal of Radioanalytical and Nuclear Chemistry* 2021 328:3. 328, 889-901 (2021). <https://doi.org/10.1007/S10967-021-07726-8>
- [54] Rycroft MJ, Nicoll KA, Aplin KL, Harrison RG. Recent advances in global electric circuit coupling between the space environment and the troposphere. *J Atmos Sol Terr Phys*. 90-91, 198-211 (2012). <https://doi.org/10.1016/j.jastp.2012.03.015>
- [55] Jeřkovský M, Javorník A, Breier R, Slučiak J, Povinec PP. Experimental and Monte Carlo determination of HPGe detector efficiency. *J Radioanal Nucl Chem*. 322, 1863-1869 (2019). <https://doi.org/10.1007/s10967-019-06856-4>
- [56] Abdolhamidzadeh B, Abbasi T, Rashtchian D, Abbasi SA. A new method for assessing domino effect in chemical process industry. *J Hazard Mater*. 182, 416-426 (2010). <https://doi.org/10.1016/j.jhazmat.2010.06.049>
- [57] Zhao Y, Nielsen CP, Lei Y, McElroy MB, Hao J. Quantifying the uncertainties of a bottom-up emission inventory of anthropogenic atmospheric pollutants in China. *Atmos Chem Phys*. 11, 2295-2308 (2011). <https://doi.org/10.5194/acp-11-2295-2011>
- [58] Aalizadeh R, Nika MC, Thomaidis NS. Development and application of retention time prediction models in the suspect and non-target screening of emerging contaminants. *J Hazard Mater*. 363, 277-285 (2019)

- [59] K lahcı F. Environmental Distribution and Modelling of Radioactive Lead (210). A Monte Carlo Simulation Application. 15-32 (2020). https://doi.org/10.1007/978-3-030-21638-2_2
- [60] Muhammad A, K lahcı F, Salh H, Hama Rashid PA. Long Short Term Memory networks (LSTM)-Monte-Carlo simulation of soil ionization using radon. *J Atmos Sol Terr Phys.* 221 105688 (2021). <https://doi.org/10.1016/j.jastp.2021.105688>
- [61] K lahcı F, Ak zcan S, G nay O. Monte Carlo simulations and forecasting of Radium-226, Thorium-232, and Potassium-40 radioactivity concentrations. *J Radioanal Nucl Chem.* 324, 55-70 (2020). <https://doi.org/10.1007/s10967-020-07059-y>
- [62] Lindmark A, Rosen B. Radon in soil gas Exhalation tests and in situ measurements. *Science of The Total Environment.* 45, 397-404 (1985). [https://doi.org/https://doi.org/10.1016/0048-9697\(85\)90243-8](https://doi.org/https://doi.org/10.1016/0048-9697(85)90243-8)
- [63] Schery SD, Gaeddert DH. Measurements of the effect of cyclic atmospheric pressure variation on the flux of 222Rn from the soil. *Geophys Res Lett.* 9, 835-838 (1982). <https://doi.org/10.1029/GL009I008P00835>
- [64] Baskaran M. Physical, Chemical and Nuclear Properties of Radon: An Introduction. *Radon: A Tracer for Geological Geophysical and Geochemical Studies.* 1-14 (2016). https://doi.org/10.1007/978-3-319-21329-3_1
- [65] Clements WE, Wilkening MH. Atmospheric pressure effects on 222Rn transport across the Earth-air interface. *Journal of Geophysical Research* (1896-1977). 79, 5025-5029 (1974). <https://doi.org/https://doi.org/10.1029/JC079i033p05025>
- [66] Nazaroff W, Nero A. Radon and its decay products in indoor air. (1988)
- [67] Tariq MA, Shah M, Hern andez-Pajares M, Iqbal T. Pre-earthquake ionospheric anomalies before three major earthquakes by GPS-TEC and GIM-TEC data during 2015–2017. *Advances in Space Research.* 63, 2088-2099 (2019). <https://doi.org/https://doi.org/10.1016/j.asr.2018.12.028>
- [68] Shah MT, Ahmad MA, Naqvi J, Jin S. Seismo ionospheric anomalies before the 2007 M7.7 Chile earthquake from GPS TEC and DEMETER. *J Geodyn.* 127, 42-51 (2019). <https://doi.org/https://doi.org/10.1016/j.jog.2019.05.004>